7-22-2019

Resonance electron interaction with five-membered heterocyclic compounds: Vibrational Feshbach resonances and hydrogen-atom stripping

Stanislav A. Pshenichnyuk

Ilya I. Fabrikant

Alberto Modelli

Sylwia Ptasińska

Alexei S. Komolov

Resonance electron interaction with five-membered heterocyclic compounds: Vibrational Feshbach resonances and hydrogen-atom stripping

Stanislav A. Pshenichnyuk,[1,*] Ilya I. Fabrikant,[2] Alberto Modelli,[3,4] Sylwia Ptasińska,[5,6] and Alexei S. Komolov[7]

[1]*Institute of Molecule and Crystal Physics, Ufa Federal Research Centre, Russian Academy of Sciences, Prospekt Oktyabrya 151, 450075 Ufa, Russia*

[2]*Department of Physics and Astronomy, University of Nebraska, Lincoln, Nebraska 68588-0299, USA*

[3]*Università di Bologna, Dipartimento di Chimica "G. Ciamician," via Selmi 2, 40126 Bologna, Italy*

[4]*Università di Bologna, Centro Interdipartimentale di Ricerca in Scienze Ambientali, via S. Alberto 163, 48123 Ravenna, Italy*

[5]*Radiation Laboratory, University of Notre Dame, Notre Dame, Indiana 46556, USA*

[6]*Department of Physics, University of Notre Dame, Notre Dame, Indiana 46556, USA*

[7]*St. Petersburg State University, Universitetskaya nab. 7/9, St. Petersburg 199034, Russia*

(Received 21 April 2019; published 22 July 2019)

Low-energy (0–15 eV) resonance electron attachment to a series of five-membered heterocyclic rings (isoxazole, imidazole, pyrazole, pyrrole, 1-methyl-, and 2-methylimidazole) is studied under gas-phase conditions by means of electron transmission spectroscopy and dissociative electron attachment spectroscopy (DEAS). Experimental spectral features are assigned on the basis of Hartree-Fock and density functional theory calculations. Sharp features, with a width of less than 0.1 eV, observed in the electron transmission spectra of imidazole, pyrazole, and pyrrole close to 0.45 eV, i.e., well below the energy of their lowest-lying π^* shape resonances detected at 1.90, 1.87, and 2.33 eV, respectively, are associated with formation of negative ion states bound by long-range electron-molecule interactions. Effective range theory calculations which include both dipolar and polarization interactions support this interpretation. In addition to the general observation of cleavage of the N–H bond at incident electron energies close to 2 eV, elimination of as many as three hydrogen atoms from the molecular negative ions is detected at higher energies by DEAS with the only exception of methylated imidazoles. This complex process is associated with ring opening and formation of diatomic hydrogen as one of the neutral fragments, as indicated by the calculations to satisfy the energetic requirements. The present results are of importance for understanding the basic mechanisms of damages caused in living tissues by high-energy radiations.

DOI: 10.1103/PhysRevA.100.012708

I. INTRODUCTION

Studies of electron-accepting properties and, in particular, dissociative electron attachment (DEA) to biologically relevant molecules representing building blocks of living matter allow us to disclose the basic mechanisms of interaction of high-energy radiations with living tissues [1–3]. Understanding these processes at the molecular level is necessary for the development of two important branches of radiobiology. The first is linked to the molecular design of pharmaceuticals and studies of natural compounds able to act as chemical protectors against ionizing radiation [4–6]. These materials can play an essential role in the complex radioprotection of humans under long-term space missions, as well as in reducing harmful effects of unwanted particle emissions or exposure to high-energy radiations in nuclear power stations [7]. The second important and rapidly growing field is linked with the properties and design of radiosensitizers used in cancer radiation (hadron) therapy [8–10]. This field is directly connected with the interactions of low-energy (0–15-eV) electrons with biorelevant molecules via resonance mechanisms [11].

Five-membered heterocyclic rings containing nitrogen or oxygen atoms, in particular pyrrole and furanlike structures, are known to be very abundant forms included as building blocks in many enzyme cofactors and natural compounds. These five-membered rings are believed to determine or enhance the pharmacological activities of molecular systems in which they are incorporated [12]. In particular, pyrazole derivatives have been found [13] to be very promising agents due to their broad pharmacological activity. The pyrazole moiety—a major pharmacophore—present in many biologically active compounds plays a vital role in diverse therapeutic properties as, for instance, anticancer activity and antiinflammatory and antibacterial effects [14,15]. Since good electron-accepting properties within the cellular environment are expected to be associated with resonance formation of molecular negative ions [16], investigations of low-energy electron-molecule interactions are of much importance for understanding about biochemical processes which take place on a molecular scale as well as for designing new therapeutic agents.

The temporary anion states of furan, pyrrole, and a series of their aza derivatives were studied earlier [17,18] by means

*Corresponding author: sapsh@anrb.ru

of electron transmission spectroscopy (ETS) [19,20] with the support of MS-Xα, MP2 and B3LYP calculations. Recently the interaction of low-energy electrons and DEA properties have been studied for isoxazole [21] and imidazole [22] using a quadrupole mass filter for separation of negative ions formed under conditions of crossed electron and molecular beams. Due to a fast evolution of the initially formed temporary negative ions (TNIs), the observation of negative species produced by DEA is very sensitive to the time scale typical of each experimental apparatus [23]. Variation of the experimental time scale can provide additional information about DEA by means of using different instruments as reported recently [24], but it is challenging to implement in a single apparatus. The present work reports DEA spectra of five-membered heterocycles obtained under different experimental conditions, namely, a different experimental time scale from those of previous studies [21,22]. In addition to imidazole and isoxazole, the series of structurally related compounds pyrazole, pyrrole, 1-methyl-, and 2-methyl-imidazole has been studied by DEA spectroscopy (DEAS) with the support of density-functional theory (DFT) calculations.

The most intriguing and unusual observation in DEA studies of imidazole and isoxazole is that of hydrogen stripping from the TNI induced by low-energy electron attachment to remove as many as three H atoms [21,22]. It was also shown that H atom stripping is accompanied by ring cleavage with formation of a negative fragment possessing a linear structure, necessary to satisfy the energetic requirements. Dehydrogenation of TNIs of biologically relevant molecules by cleavage of N–H or O–H bond is generally observed around 1–2 eV, whereas cleavage of C–H bonds usually requires much more energy. In fact, DEA to many molecules with biological activity is dominated by formation of $[M-\mathrm{H}]^-$ (where M stands for a target parent molecule) closed-shell anions at incident electron energies around 1 eV [25–30]. Elimination of two hydrogen atoms from the molecular anion was observed in the DEA spectra of indole and related molecules [27], polyphenolic compounds [31], and other molecules able to form new more stable structures [32]. The present research provides some insight into this interesting phenomenon.

Another aspect of the present study is linked with the possibility to form dipole-bound anion states (DBSs) [33,34]. Desfrançois and co-workers [33,35], by analyzing binding energies and dipole moments of various molecules, concluded that dipole-bound anion states exist if the dipole moment exceeds the so-called critical value (2.5 D [36]). In fact, the critical dipole moment for a stationary dipole is much lower, 1.625 D, which could be relevant to heavier molecules where the rotational effects are not essential. Several molecules whose dipole moment is close to this value or even lower support vibrational Feshbach resonances (VFRs) which are quasibound states in the field of the vibrationally excited molecule. A good example is the methyl iodide molecule whose dipole moment is 1.62 D and which exhibits a very pronounced VFR below the first excitation threshold of the C–I stretch vibrations [37,38]. In this case, like in many other examples relevant to halogen-containing molecules [2,39,40] the existence of weakly bound states depends on several other factors including short-range forces and the polarization interactions. Later, sharp structures in the total scattering cross sections [41] and DEA cross sections [25] of halouracils were ascribed [41] to VFRs which in this case are essentially due to dipole-supported states because of the large dipole moments of these compounds. Recently, it has been suggested that DEA to formamides can proceed via formation of dipole-support core-excited resonances that correlate with both singlet and triplet excited states of neutral molecules [42].

In the present work, we describe studies of the total scattering cross section of a number of five-membered heterocyclic compounds in which sharp structures appear at energies very close to the first N–H stretching vibrational excitation. These structures are in fact observed in compounds which contain an N–H group, namely, pyrazole, imidazole, pyrrole, but not in isoxazole, where this vibrational mode is not present. This work was stimulated in part by a trapped electron study [43] of pyrazole, in which attachment of electrons was observed at 0.75 eV, far below the energy (1.89 eV) of the lowest-lying shape resonance [18]. In contrast, the spectrum of isoxazole obtained with the same experimental technique displays the lowest peak at about 1 eV [44], i.e., very close to the first valence anion produced by vertical electron attachment at 1.09 eV [18]. In the present work we also show that formation of VFRs in pyrazole and pyrrole as observed in ETS are not due to the purely dipolar interaction but can be affected by polarization of the target molecule as discussed earlier [37,45,46].

II. EXPERIMENTAL AND COMPUTATIONAL METHODS

A. Electron transmission spectroscopy

The ETS apparatus is in the format devised by Sanche and Schulz [19], and the detailed experimental conditions were described earlier [20,47]. Briefly, a magnetically collimated electron beam of well-defined energy was passed through a collision cell containing a vapor of the substance under investigation. The transmitted electron current was collected. To enhance resonant structures in the total electron scattering cross section, the first derivative of the electron current transmitted through the gas sample was measured with a synchronous lock-in amplifier. Each resonance, associated with the formation of a TNI, is characterized by a minimum and a maximum in the derivative signal. The energy of the midpoint between these features is assigned to the vertical attachment energy (VAE). The electron energy scale was calibrated by an admixture of N_2 gas, referring to the sharp structures related to formation of the N_2^- ($^2\Pi_g$) state. The corresponding extrema in the derivative signal are found to be at 1.98, 2.22, 2.46, and 2.69 eV. The estimated accuracy of the measured VAEs is ± 0.05 eV. A trochoidal electron monochromator in the format devised by Stamatovic and Schulz [48] was used to achieve an electron energy resolution of 50 meV [full width at half maximum (FWHM)].

B. Dissociative electron attachment spectroscopy

A general overview of DEAS may be found elsewhere [49–53]. Our 90°-magnetic sector mass spectrometer has been described in detail previously [50]. A schematic representation and description of specific conditions may be found

elsewhere [54]. Briefly, a magnetically collimated electron beam with defined energy was passed through a collision cell containing a vapor of the substance under investigation, under single-collision conditions. Currents of mass-selected negative ions formed by DEA were recorded as a function of the incident electron energy in the 0–14-eV energy range. The electron energy scale was calibrated with the SF_6^- signal at zero energy, generated by attachment of thermal electrons to SF_6. The FWHM of the electron energy distribution was 0.4 eV, and the accuracy of the measured peak positions was estimated to be ±0.1 eV. The substances under investigation are commercially available from Sigma-Aldrich and were used without further treatment or additional purification.

C. Quantum chemical calculations

To assign features found in the total electron scattering cross section to resonant states associated with occupation of normally empty molecular orbitals, *ab initio* Hartree-Fock calculations were performed using the GAMESS [55] quantum chemical package. The 6-31G(d) basis set was used for optimization of the geometry of the neutral molecules and for calculation of virtual orbital energies (VOEs). The VAEs measured in various families of compounds were found to be linearly correlated with the corresponding VOEs of the neutral molecules calculated with basis sets which do not include diffuse functions [56–58].

In this work, the π^* VAEs were predicted by scaling the HF/6-31G(d) VOEs with the equation obtained for a series of alternating phenyl and ethynyl groups [59]: VAE = [VOE−2.22]/1.69. To scale σ^* VOEs, the relationship VAE = [VOE−2.856]/1.096 found for σ^* (C–Cl) resonances of chloroalkanes [47] was employed. The latter scaling is thus expected to give a larger error, the σ^* (C–Cl) orbitals being not present in the molecules under investigation. The vertical electron affinity (EA_v) was calculated as the difference between the total energy of the neutral and the lowest anion state, both in the optimized geometry of the neutral state, using the B3LYP functional and the standard 6-31+G(d) basis set (which includes the minimum addition of diffuse functions). The adiabatic electron affinity (EA_a) was obtained as the energy difference between the neutral and the lowest anion state, each in its optimized geometry.

To assign the structures of the fragments observed in DEA spectra, the thermodynamic energy thresholds are calculated as the difference between total energies of the negatively charged and neutral fragment species and that of the neutral ground state at the B3LYP/6-31+G(d) level of theory using the GAUSSIAN09 set of programs [60].

D. Effective range theory with complex boundary conditions

Multichannel effective range theory (ERT) is a limiting case of the *R*-matrix theory as described earlier in the description of slow electron-SF_6 scattering [61,62]. Application of this approach to reproduce experimental features in low-energy DEA to iron pentacarbonyl, $Fe(CO)_5$, as well as the detailed description of the calculation procedure can also be found elsewhere [63]. Long-range electron-molecule interactions strongly influence the low-energy scattering. In this case a virtual or "slightly unbound" state can be formed and described in terms of the scattering theory [64] in the framework of the ERT earlier [62]. Briefly, at the first stage the incoming electron influences the nuclei by coupling to a symmetric N–H stretch motion (in compounds containing this bond) with simultaneous capture. The excess energy deposited by the electron is channeled either into breaking the N–H bond and elimination of a neutral H atom, or into electron detachment. ERT has demonstrated its capacity to describe the subtleties of extremely short-lived anion states and the transition region from the virtual state into the bound state [65].

III. RESULTS AND DISCUSSION

A. Shape resonances in the total scattering cross section

Electron transmission (ET) spectra for isoxazole (I), imidazole (II), pyrazole (III), and pyrrole (IV) are dominated by the π^* resonant states [18], but the cusp features were not reported. Here we report observation of these rather unusual spectral structures for the five-memeberd heterocyclic compounds (II–IV) which contain an NH group. The most intense signals in the present ET spectra can be ascribed to formation of π^* shape resonances (SRs) [49] associated with occupation of the lowest valence π^* molecular orbitals (MOs) as shown in Fig. 1. The heterocyclic ring of compounds I–IV (see structures in Fig. 1) includes two C=C or C=N double bonds, therefore the ET spectrum is expected to display two intense π^* SRs, marked as π_1^* and π_2^* in Fig. 1 and reported in Table I. Vertical electron attachment to the lowest unoccupied MO (LUMO) and the second empty π^* MO of I are detected at 1.09 and 2.74 eV, respectively, in quite close agreement with the previously reported data [18]. The measured VAEs for I–IV are in good agreement with the scaled HF/6-31G(d) VOEs presented in Table I. More results on π^* resonances for compounds I–IV including their assignment based on MP2/6-31G(d) and B3LYP/6-31G(d) calculations can be found elsewhere [18].

The following discussion about coupling of DBS with valence σ^* TNIs requires summarizing very few data about σ^*_{N-H} states in compounds II–IV. Although the σ^*_{N-H} SRs associated with very short-lived TNI states are not observed in the ET spectra, the corresponding VAEs are tentatively predicted to lie at 2.86, 3.04, and 3.03 eV in II–IV, respectively, by means of the scaling procedure as described above. Therefore, the expected weak and broad signals associated with the σ^*_{N-H} states can be obscured in the ET spectra by the presence of the π_2^* resonances, ranging from 2.74 to 3.44 eV in II–IV. A schematic representation of the σ^*_{N-H} virtual MO in II–IV is shown in Fig. 2. This MO, with essentially the same shape in compounds II–IV, possesses antibonding character with respect to the ring and is mainly located on the N_1-H bond.

B. Cusp features and VFRs in the total scattering cross section

Sharp signals appearing in the ETS spectra of a series of halouracils at low energy and associated with formation of VFRs have been reported by Scheer *et al.* [41]. An interesting observation of the present work is detection of a similar

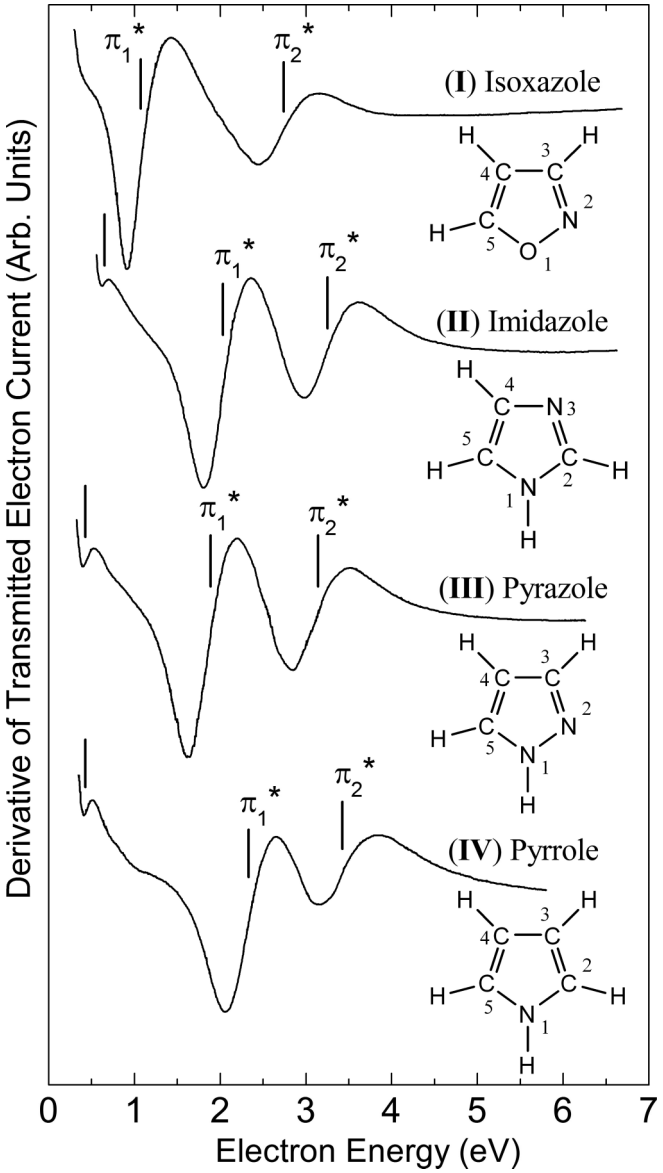

FIG. 1. First derivative of the electron current transmitted through gas-phase samples of compounds I–IV as a function of incident electron energy. Vertical bars mark the measured energies of vertical electron attachment. Negative-ion states associated with occupation of the lowest π^* orbitals are indicated. The sharp features appearing close to 0.45 eV for compounds II–IV are ascribed to formation of vibrational Feshbach resonances.

feature far below the lowest π^* resonance in compounds II–IV, possessing a FWHM (measured as dip-to peak separation) smaller than 0.1 eV, see Table I, as compared with that (about 0.5 eV) of the π^* SRs. These narrow signals are displayed in the ET spectra of compounds II–IV at electron energies around 0.45 eV, as indicated in Fig. 1 by vertical bars and listed in Table I. It is expected that similarly to substituted uracils [41] these sharp features are due to symmetry allowed mixing of dipole-assisted anion states with valence states associated with a low-lying σ^*_{N-H} MO. Careful analysis down to low incident electron energies has shown that a corresponding sharp structure is not present in the ET spectrum of isoxazole

TABLE I. Measured VAEs, dip-to-peak separations (in parentheses), HF/6-31G(d) VOEs, and their scaled values (SVOEs) in a series of five-membered heterocyclic compounds. All values are in eV. Cusp features are marked in bold.

Orbital	VOE	SVOE	VAE (FWHM)
		(I) Isoxazole	
σ^*	7.077	3.82	
π_2^*	6.372	2.46	2.74 (0.68)
π_1^*	4.027	1.07	1.09 (0.49)
		(II) Imidazole	
σ^*	7.771	4.44	
π_2^*	6.822	2.72	3.16 (0.65)
σ^*_{N-H}	6.014	2.86	
π_1^*	5.349	1.85	1.90 (0.54)
			0.46 (0.08)
		(III) Pyrazole	
σ^*	7.754	4.43	
π_2^*	6.806	2.71	3.14 (0.67)
σ^*_{N-H}	6.212	3.04	
π_1^*	5.050	1.67	1.87 (0.58)
			0.44 (0.09)
		(IV) Pyrrole	
σ^*	7.959	4.61	
π_2^*	7.205	2.95	3.44 (0.65)
σ^*_{N-H}	6.199	3.03	
π_1^*	5.664	2.04	2.33 (0.58)
			0.44 (0.09)
		(V) 1-Methylimidazole	
σ^*	7.399	4.11	
π_2^*	6.800	2.71	
π_1^*	5.234	1.78	
		(VI) 2-Methylimidazole	
σ^*	7.307	4.03	
π_2^*	6.960	2.80	
σ^*_{N-H}	5.989	2.84	
π_1^*	5.330	1.84	

(see Fig. 1). This finding is in line with the absence of N–H bonds in molecule I, so that mixing of a DBS with a low-energy σ^* valence state is not possible.

In contrast to thymine, uracil, and halouracils [25,41], in the present case only imidazole possesses a permanent dipole moment larger than 2.5 D to support formation of dipole-bound anions (see Table II). However, as discussed

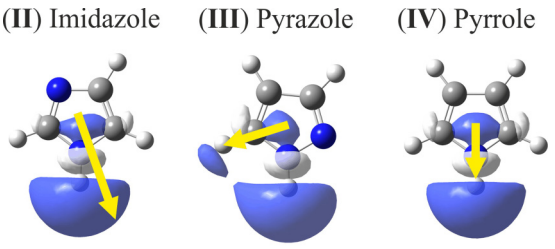

FIG. 2. Schematic representations of σ^*_{N-H} virtual molecular orbitals in II–IV. Direction and magnitude of the dipole moments calculated at the B3LYP/6-31+G(d) level are schematically indicated by the yellow arrows.

TABLE II. Experimental values of dipole moments (derived from the gas-phase microwave spectra), polarizabilities (from the measurements in dioxan solutes), and vibrational frequencies (from the gas-phase IR spectra) for molecules II–IV.

Dipole moment (Debye)	Polarizability (Å^3) [70]	Frequency (cm^{-1})
	(II) Imidazole	
3.667 ± 0.05 [67]	7.41	3518 [71]
	(III) Pyrazole	
2.214 ± 0.015 [68]	7.54	3523 [72]
	(IV) Pyrrole	
1.74 ± 0.02 [69]	8.27	3531 [73]

in the Introduction, weakly bound states and VFRs can exist in systems whose dipole moment is well below the critical value [37,46] since VFRs and threshold cusps in vibrational excitation and, in particular, DEA cross sections are strongly affected by polarization of the target molecule [46]. Indeed, in the present series pyrrole possesses the lowest permanent dipole moment (1.74 D), i.e., much below the critical value, but its polarization exceeds that of molecules II and III. Therefore, VFRs in IV are expected to be formed with involvement of a bound anion state due to induced attraction, since in the present case the experimental feature lies below the threshold for vibrational excitation [46,66]. It is also worth mentioning that according to B3LYP/6-31+G(d) calculations the permanent dipole moment in pyrrole is aligned along the N–H bond as shown in Fig. 2. Therefore, a better mixing of the dipole-supported anion state with the lowest valence σ^*_{N-H} resonance is expected in molecule IV despite its smaller dipole moment. This mixing is also enhanced by the partial valence character of DBS wave function [25]. Due to the presence of an additional nitrogen atom in their five-membered rings, the direction of the dipole moments of imidazole and pyrazole does not coincide with that of the N–H bond, thus reducing the mixing in comparison with pyrrole.

To support these qualitative considerations, we performed ERT calculations of the DEA cross section for electron scattering by molecules II–IV below 1 eV. Experimental values for dipole moments [67–69], polarizabilities [70], and vibrational quanta associated with the N–H stretching vibration [71–73] in II–IV were used as the input parameters, as listed in Table II. The same short-range parameters were used for the three compounds. The results are presented in Fig. 3. The most pronounced cusp feature is calculated in the electron attachment cross section of imidazole, likely due to its higher permanent dipole moment. However, even the lowest value of dipole moment is predicted to give rise to a cusp in the cross section of pyrrole. This feature is more intense than that of pyrazole likely due to the highest polarizability of molecule IV. Some discrepancy between the energy positions of the cusps in ET spectra and in the calculated curves can be due to superposition of the experimental features with the right wing of the intense electron beam signal [20], in addition to possible inaccuracy of the ERT model for describing short-range interactions. We therefore assign the sharp features

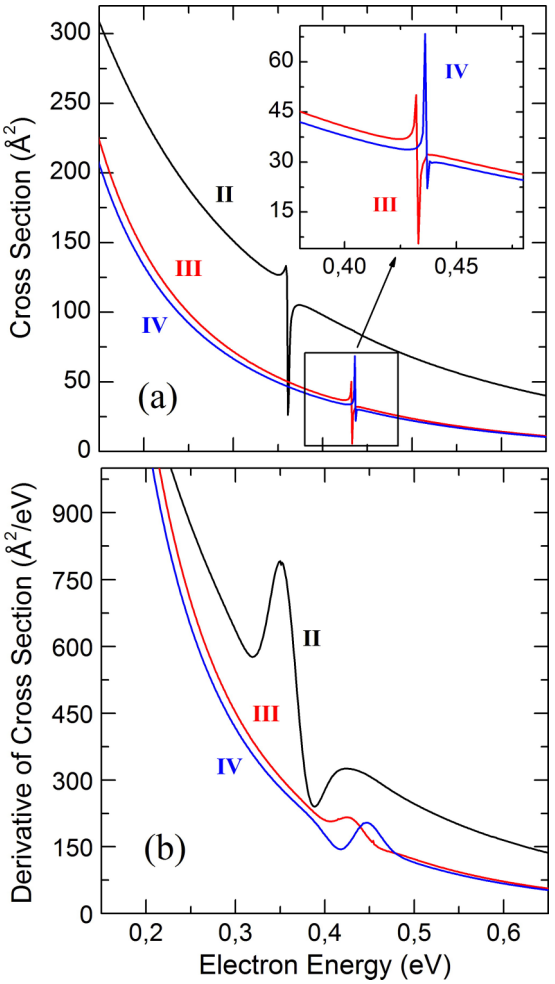

FIG. 3. Calculated electron scattering cross section (a) and the first derivative of its averaged value (b) as a function of incident electron energy for imidazole (II, black line), pyrazole (III, red line), and pyrrole (IV, blue line).

observed around 0.45 eV in II–IV to formation of VFRs associated with mixing between a valence σ^*_{N-H} resonance and dipole-supported anion states, in analogy with the earlier observations in thymine and halogenated uracils [25,41].

C. Single H atom elimination from TNIs

Currents of mass-selected negative ions formed by gas-phase DEA to compounds I–IV as well as to 1-methylimidazole (V) and 2-methylimidazole (VI; see structures reported in Fig. 6) are presented in Figs. 4–6 as a function of incident electron energy in order of decreasing intensity of the signals. These data are summarized in Table III, in order of decreasing mass number. To support the structures proposed for the fragment species formed by low-energy electron attachment to compounds I–VI, Table IV shows the B3LYP/6-31+G(d) thermodynamic energy thresholds for formation of specified fragments, including proposed structures for the neutral species. With the only exception of V, elimination of a neutral H atom is found to be the most intense decay channel of the parent molecular anions formed with the lowest π^*_1 resonances.

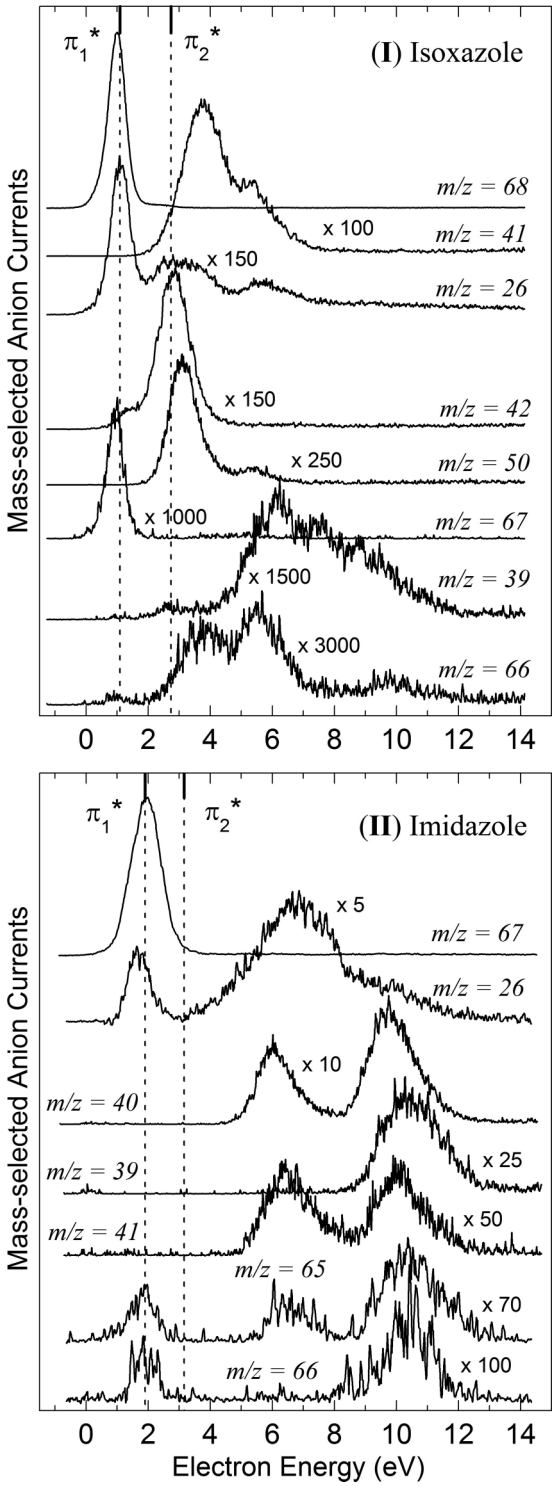

FIG. 4. Currents of mass-selected negative ions formed by DEA to gas-phase samples of compounds I and II as a function of incident electron energy. The signals are arranged in order of decreasing intensity. Measured positions of the lowest π_1^* and π_2^* shape resonances are indicated by vertical dashed lines.

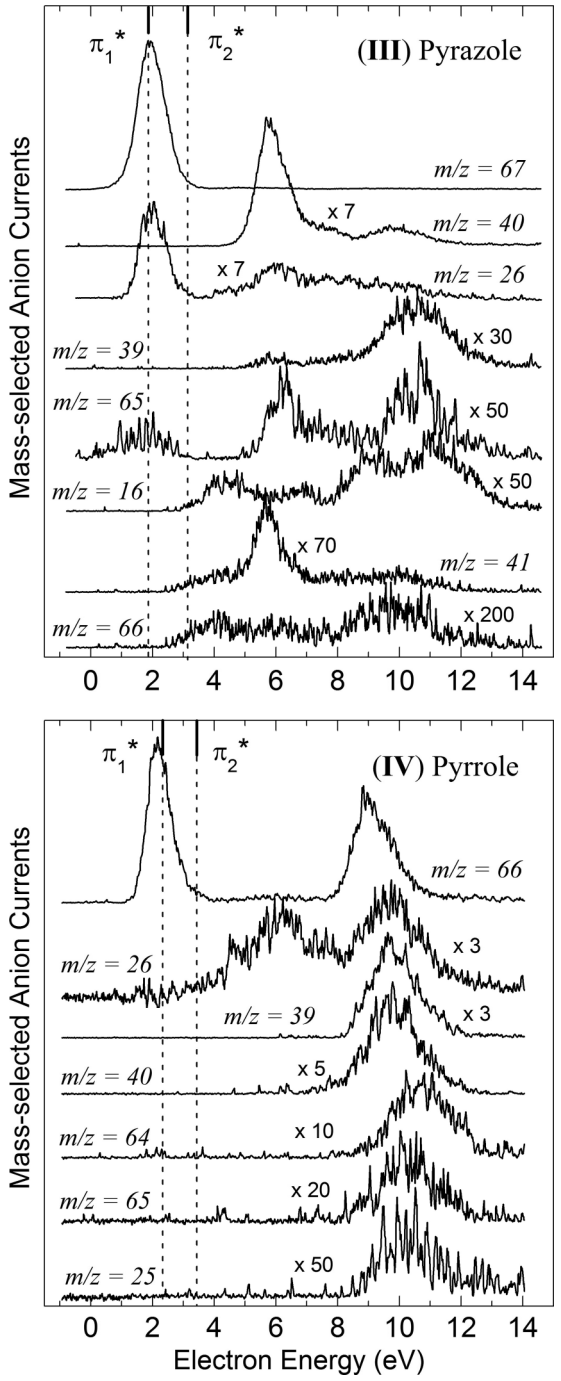

FIG. 5. Currents of mass-selected negative ions formed by DEA to gas-phase samples of compounds III and IV as a function of incident electron energy. The signals are arranged in order of decreasing intensity. Measured positions of the lowest π_1^* and π_2^* shape resonances are indicated by vertical dashed lines.

In spite of the absence of N–H bonds in isoxazole, the $[I-H]^-$ ion ($m/z = 68$ in Fig. 4) is unexpectedly observed at low electron energy (1.0 eV). In contrast, in this regard, molecule V fulfills expectations, i.e., there is no low-energy signal in the $[V-H]^-$ current ($m/z = 81$ in Fig. 6). Indeed, according to the present calculations direct elimination of a H atom from the ring in I–VI (or the methyl group in V and VI) requires incident electron energies in the 2.5–3.9-eV range (see Table III). However, according to the present B3LYP/6-31+G(d) results, this DEA channel is energetically favored when elimination of the H atom bonded to C(3) (position

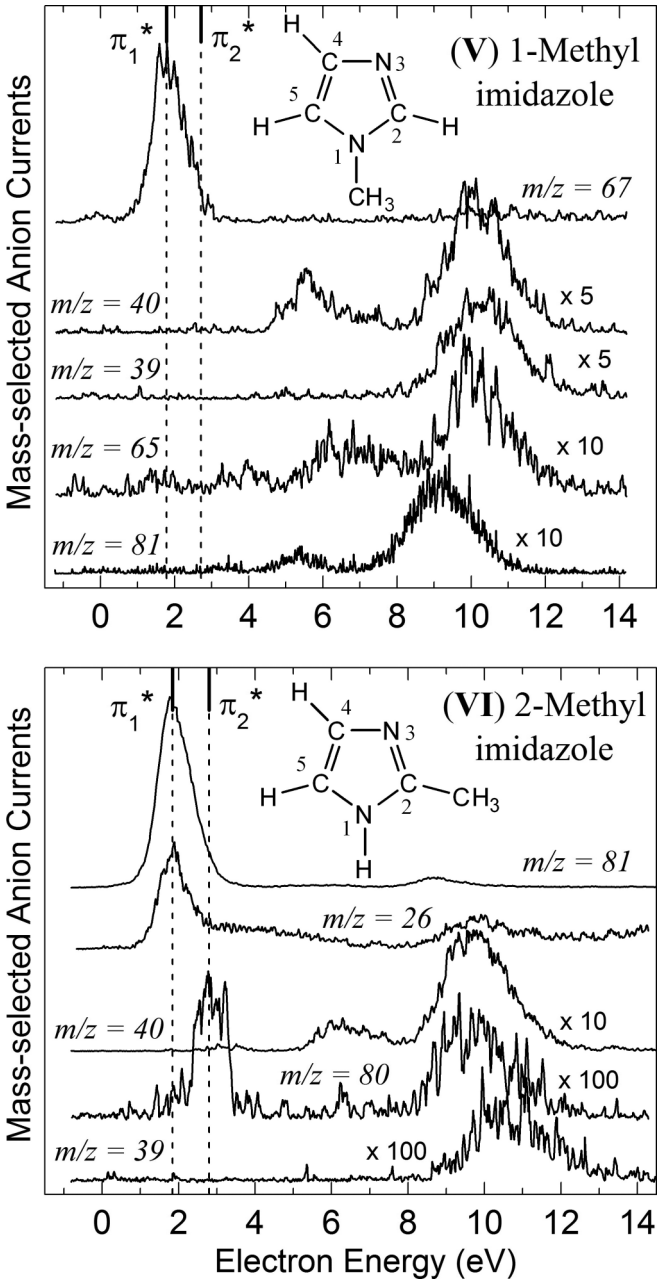

FIG. 6. Currents of mass-selected negative ions formed by DEA to gas-phase samples of compounds V and VI as a function of incident electron energy. The signals are arranged in order of decreasing intensity. Molecular structures for V and VI are reported. Predicted positions of the lowest π_1^* and π_2^* shape resonances are indicated by vertical dashed lines.

labels are given in Fig. 1) from the I^- molecular anion is accompanied by opening of the ring via cleavage of the O(1)–N(2) bond and rearrangement of the anion to give structure Ia (see Fig. 7). The corresponding thermodynamic threshold is predicted to be negative (−0.24 eV with inclusion of zero-point vibrational energy corrections; see Table III). In agreement, in the optimized geometry of anion I^- the O(1)–N(2) bond is calculated to be elongated to 1.465 Å [with simultaneous out-of-plane bending of the C(5)–H bond], to be compared with 1.401 Å in neutral isoxazole. The proposed

TABLE III. Possible structures of anionic fragments generated by DEA in a series of five-membered heterocyclic compounds, peak energies (eV), and relative intensities (taken from the peak heights).

M/z	Anion structure	Peak energy[a]	Relative intensity
		(I) Isoxazole	
68	$[I-H]^-$	1.0	100
67	$[I-2H]^-$	1.0	0.1
66	$[I-3H]^-$	1.1	<0.1
		3.8	<0.1
		5.5	<0.1
		9.8	<0.1
50	$[I-2H-OH]^-$	3.0	0.3
		5.3 sh.	
42	OCN^-	1.3 sh.	
		2.8	0.6
41	$[I-CO]^-$	3.8	0.9
		5.3 sh.	
39	$[I-2H-CO]^-$	2.7	<0.1
		6.2	<0.1
		7–8 sh.	
26	CN^-	1.1	0.6
		3.0	0.2
		5.7	0.1
		(II) Imidazole	
67	$[II-H]^-$	2.0	100
66	$[II-2H]^-$	1.9	0.3
		10.3	0.4
65	$[II-3H]^-$	1.9	0.7
		6.5	0.4
		10.3	0.9
41	$[II-CNH]^-$	6.4	1.0
		10.0	1.2
40	$[II-CHNH]^-$	6.0	4.9
		9.8	7.2
39	$[II-CH_2NH]^-$	10.4	2.2
26	CN^-	1.8	8.3
		6.8	15
		∼10 sh.	
		(III) Pyrazole	
67	$[III-H]^-$	2.0	100
66	$[III-2H]^-$	∼4–6	
		9.7	0.1
65	$[III-3H]^-$	1.7	0.3
		6.3	1.0
		10.5	1.0
41	$[III-CNH]^-$	4.0 sh.	
		5.7	0.4
40	$[III-CHNH]^-$	5.8	12
		7.7 sh.	
		9.9	1.8
39	$[III-CH_2NH]^-$	5.9	0.2
		10.5	1.4
26	CN^-	2.0	8.9
		5.9	3.5
		∼8–10	
16	NH_2^-	4.5	0.4
		9.1 sh.	
		11.0	0.9

TABLE III. *(Continued).*

M/z	Anion structure	Peak energy[a]	Relative intensity
	(IV) Pyrrole		
66	$[IV-H]^-$	2.1	100
		8.9	65
65	$[IV-2H]^-$	10.3	1.9
64	$[IV-3H]^-$	10.7	4.3
40	$[IV-CH_2CH]^-$	9.8	9.1
39	$[IV-C_2H_4]^-$	9.8	21
26	CN^-	6.1	25
		9.7	23
25	C_2H^-	∼10	0.6
	(V) 1-Methylimidazole		
81	$[V-H]^-$	5.3	1.0
		9.2	6.5
67	$[V-CH_3]^-$	1.8	100
65	$[V-2H-CH_3]^-$	6.7	2.6
		10.1	8.7
40	$[V-CHNCH_3]^-$	5.5	8.7
		10.1	17
39	$[V-CH_2NCH_3]^-$	10.3	13
	(VI) 2-Methylimidazole		
81	$[VI-H]^-$	1.8	100
		8.7	5.2
80	$[VI-2H]^-$	2.9	0.6
		9.8	0.3
40	$[VI-CH_3CNH]^-$	6.1	1.3
		9.7	6.8
39	$[VI-CH_3CH_2N]^-$	10.4	0.4
26	CN^-	1.8	55
		9.9	17

[a]sh. means shoulder.

TABLE IV. B3LYP/6-31+G(d) total energies (eV) relative to the neutral ground state. The values in parentheses are corrected for zero-point vibrational energies.

M/z	Fragments (anion + neutral)		Total energy
	(I) Isoxazole		
68	$[I-H(3)^a]^- + H^\bullet$	Ia[b]	0.18 (−0.24)
68	$[I-H(4)]^- + H^\bullet$		3.29 (2.92)
68	$[I-H(5)]^- + H^\bullet$		2.96 (2.56)
67	$[I-2H(3,5)]^- + H_2$	Ib	−0.68 (−1.16)
67	$[I-2H(3,4)]^- + H_2$		0.07 (−0.44)
66	$[I-3H]^- + H_2 + H^\bullet$	Ic	1.35 (0.63)
50	$CCCN^- + H_2 + HO^\bullet$		3.11 (2.45)
42	$OCN^- + H_2C=CH^\cdot$		−0.07 (−0.36)
41	$H_2CC(H)N^- + CO$		0.80 (0.46)
39	$HCCN^- + H_2 + CO$		1.42 (0.74)
26	$CN^- + H_2CC(H)O^\bullet$		−0.05 (−0.34)
	(II) Imidazole		
67	$[II-H(1)]^- + H^\bullet$		1.76 (1.39)
67	$[II-H(2)]^- + H^\bullet$		3.59 (3.19)
67	$[II-H(4)]^- + H^\bullet$		4.26 (3.83)
67	$[II-H(5)]^- + H^\bullet$		3.48 (3.10)
66	$[II-2H(1,2)]^- + H_2$		2.07 (1.62)

TABLE IV. *(Continued).*

M/z	Fragments (anion + neutral)		Total energy
66	$Malononitrile^- + H_2$		1.85 (1.29)
65	$[II-3H(1,2,5)]^- + H_2 + H^\bullet$		7.47 (6.61)
65	$[Malononitrile-H]^- + H_2 + H^\bullet$		2.72 (1.91)
41	$HCCNH_2^- + HCN$		3.88 (3.48)
40	$HCCNH^- + H_2C=N^\bullet$		3.53 (3.10)
39	$HCCN^- + H_2CNH$		2.51 (2.15)
26	$CN^- + CH_3C(H)N^\bullet$		1.30 (0.99)
	(III) Pyrazole		
67	$[III-H(1)]^- + H^\bullet$		2.02 (1.62)
67	$[III-H(3)]^- + H^\bullet$		4.09 (3.65)
67	$[III-H(4)]^- + H^\bullet$		3.89 (3.49)
67	$[III-H(5)]^- + H^\bullet$		3.33 (2.95)
66	$[III-2H(3,5)]^- + H_2$	IIIa	1.25 (0.70)
66	$[III-2H(1,5)]^- + H_2$		2.31 (1.84)
65	$[III-3H(1,3,5)]^- + H_2 + H^\bullet$	IIIb	2.28 (1.47)
41	$C_2H_3N^- + HCN$		2.26 (1.82)
40	$H_2C=C=N^- + HC=NH^\bullet$		2.21 (1.79)
39	$HCCN^- + H_2CNH$		2.07 (1.70)
26	$CN^- + CH_3C(H)N^\bullet$		0.86 (0.55)
16	$NH_2^- + NCCHCH^\bullet$		4.34 (3.90)
	(IV) Pyrrole		
66	$[IV-H(1)]^- + H^\bullet$		2.20 (1.81)
66	$[IV-H(2)]^- + H^\bullet$		3.86 (3.46)
66	$[IV-H(3)]^- + H^\bullet$		4.32 (3.90)
65	$[IV-2H(1,2)]^- + H_2$		2.45 (1.98)
65	$Cyanopropyne^- + H_2$	IVa	2.38 (1.84)
64	$[IV-3H(1,2,5)]^- + H_2 + H^\bullet$		7.67 (6.81)
64	$[Cyanopropyne-H]^- + H_2 + H^\bullet$	IVb	4.44 (3.59)
40	$H_2C-CN^- + H_2C=CH^\bullet$		3.08 (2.65)
40	$H_2C=C=CH_2^- + HCN$		3.28 (2.82)
39	$HCCN^- + H_2C=CH_2$		2.28 (1.92)
26	$CN^- + H_2C=CH-CH_2^\bullet$		1.21 (0.90)
25	$C_2H^- + H_2C=CH-NH^\bullet$		3.91 (3.53)
	(V) 1-Methylimidazole		
81	$[V-H(CH_3)]^- + H^\bullet$		3.62 (3.20)
81	$[V-H(2)]^- + H^\bullet$		3.59 (3.18)
81	$[V-H(4)]^- + H^\bullet$		4.31 (3.88)
81	$[V-H(5)]^- + H^\bullet$		3.49 (3.10)
67	$[V-CH_3]^- + CH_3^\bullet$		0.95 (0.62)
65	$[V-2H(2,5)-CH_3]^- + H_2 + CH_3^\bullet$		6.65 (5.85)
65	$[V-2H(2,5)-CH_3]^- + CH_4 + H^\bullet$		6.58 (5.91)
65	$[Malononitrile-H]^- + CH_4 + H^\bullet$		1.83 (1.21)
40	$HC\equiv C-NH^- + HC=NCH_3^\bullet$		3.95 (3.56)
39	$HCCN^- + H_2C=NCH_3$		2.43 (2.08)
26	$CN^- + H_2C=CH-CH_2-NH^\bullet$		2.22 (1.89)
26	$CN^- + H_3C-CH=CH-NH^\bullet$		1.23 (0.93)
	(VI) 2-Methylimidazole		
81	$[VI-H(1)]^- + H^\bullet$		1.84 (1.45)
81	$[VI-H(CH_3)]^- + H^\bullet$		3.43 (3.00)
81	$[VI-H(4)]^- + H^\bullet$		4.34 (3.90)
81	$[VI-H(5)]^- + H^\bullet$		3.56 (3.18)
80	$[VI-2H(1,CH_3)]^- + H_2 + H^\bullet$		0.93 (0.48)
40	$H_2C=CN^- + CH_3C=NH^\bullet$		2.49 (2.12)
39	$HC-CN^- + H_3C-CH-NH$		2.42 (2.08)
26	$CN^- + H_3C-CH=CH-NH^\bullet$		1.52 (1.23)

[a]Atom positions are indicated in parentheses according to the labeling reported in Fig. 1.

[b]Structures are presented in Fig. 7.

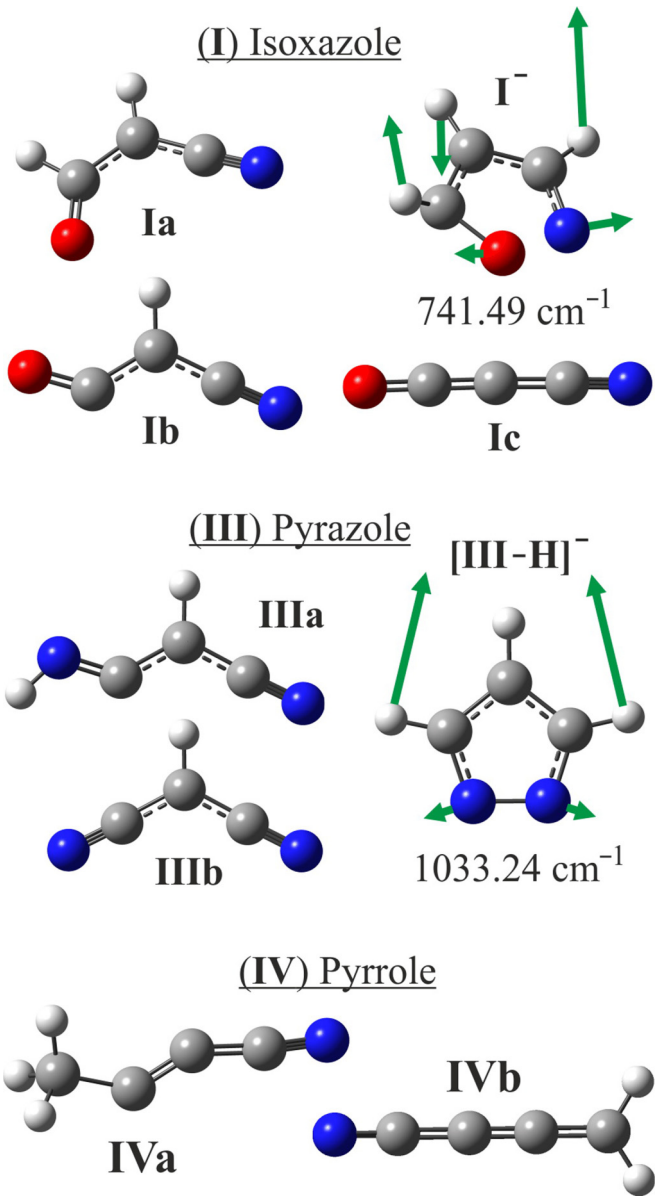

FIG. 7. Proposed structures of some anionic fragments formed by gas-phase DEA to compounds I–IV and characteristic vibrational modes of some anionic species calculated at B3LYP/6-31+G(d) level of theory.

ring opening of the I^- molecular anion can represent a precursor state for a variety of DEA channels. It can be suggested that electron attachment to I initiates a characteristic out-of-plane vibration (fifth normal mode, with a calculated frequency of 741.40 cm^{-1}; the displacement vectors are displayed in Fig. 7) of the isoxazole ring that simultaneously elongates the O(1)–N(2) bond and stimulates elimination of H atom(s), especially from the C(3) position since its displacement is predicted to be the largest. A similar finding was reported recently showing that the most dominant DEA pathway in isoxazole occurs through the loss of hydrogen at C(3), which leads to ring opening by O–N bond cleavage [21]. A previous work reported a resonance structure for the $[I-H]^-$ ion at an energy of ~1.5 eV, which is in agreement to the present study within an electron-beam resolution of experimental apparatus [21].

It is also worth mentioning that selective deprotonation of oxazole (not studied in this work), where in contrast to I the two ring heteroatoms are separated by a carbon atom, via slow secondary electron attachment leads to production of an oxazolide anion with its cyclic structure (the EA_a of the corresponding neutral oxazolyl σ radical being estimated to be 2.21 eV) as shown by anion photoelectron imaging spectroscopy [74]. Our attempts to find an open structure for the dehydrogenated anion of compound V characterized by a DEA threshold below 2 eV were unsuccessful. In agreement, the $[V-H]^-$ current displays peaks only at high energies (5.3 and 9.2 eV), ascribed to core-excited states [49]. It can therefore be concluded that, at least in the present case, opening of the five-membered cycle occurs via cleavage of the covalent bond between adjacent heteroatoms.

The $[I-H]^-$ current peaks at 1.0 eV, i.e., very close to the VAE (1.09 eV) of the lowest π^* shape resonance observed in ETS (see Fig. 4). Therefore, dehydrogenation of isoxazole by DEA is attributed to the well-known mechanism found for planar unsaturated hydrocarbons [75,76]. This mechanism consists in initial formation of a π^* TNI, followed by π^*/σ^* coupling due to out-of-plane vibration which allows H atom elimination via a repulsive σ^* state. In this case the maximum anion yield is observed very close to the energy of the corresponding π^* resonance. Since low-lying σ^* MOs are not expected in I, the alternative direct DEA mechanism occurring through a σ^* resonance [77] can be ruled out.

By analogy to the case of halogenated uracils [41], a distinct dissociation mechanism associated with formation of a dipole-supported anion state and VFRs observed around 0.45 eV by ETS can be invoked for II–IV and VI. Indeed, in uracil the VFR was observed around 0.4 eV [41], but the most intense peak in the $[U-H]^-$ (U = uracil) current lies at 1.01 eV, i.e., associated with the third vibrational level of DBS. A less intense sharp feature in the $[U-H]^-$ current detected at 0.69 eV was ascribed by the second vibrational level of DBS, whereas the first one is expected to lie below the DEA threshold and cannot contribute to the $[U-H]^-$ signal [41]. In the present case, abstraction of a hydrogen atom (or CH_3 group in V) from the N(1) site in compounds II–IV and VI is energetically allowed below 2 eV (see Table III), so that ring opening is likely not involved in formation of the observed $[M-H]^-$ (or $[M-CH_3]^-$) anions. They can be due to formation of VFRs via coupling of a DBS with a valence σ^* anion state that initiates H atom tunneling through the potential barrier formed by avoided crossing between these states [25]. The same mechanism is attributed to dehydrogenation of several amino acids via the DEA [78,79]. However, in the present case the position of the lowest π_1^* resonance matches well the observed maxima of the $[M-H]^-$ DEA signals ($m/z = 67$ for II and III, $m/z = 66$ for IV, and $m/z = 81$ for VI, as shown in Figs. 4–6) that makes it difficult to identify the exact mechanism of H atom abstraction. It is to be noted that the most intense DEA channel in V is due to excision of a methyl group from N(1), leading to the $[V-CH_3]^-$ negative fragment ($m/z = 67$ in Fig. 6), formed by dissociation of the lowest π_1^* shape resonance.

D. H atom stripping

Abstraction of two H atoms from the molecular TNI, accompanied by formation of hydrogen molecule as a neutral counterpart to satisfy the energetic conditions, was found to be a characteristic decay channel in DEA to polyphenolic compounds, associated with cleavage of O–H bonds [31,80,81]. Formation of $[M-2H]^-$ and H_2 fragments is also in agreement with the DEA spectra of amino acids such as valine, β-alanine, and glycine [82–84]. More recently abstraction of two and three H atoms, referred to as H atom striping, was detected in DEA to imidazole, isoxazole, indole, and related molecules, accompanied by strong structural rearrangements, including ring opening [21,22,27]. In the present case both DEA channels, $[M-2H]^-$ and $[M-3H]^-$, are detected with low intensities in compounds I–IV (see Figs. 4 and 5 and Table III).

Considering the characteristic vibration of the isoxazole anion reported in Fig. 7, it can be suggested that two hydrogen atoms at the C(3) and C(5) sites can be eliminated in the same direction, thus favoring formation of an H_2 molecule as a neutral fragment. Indeed, the $[I-2H]^-$ species with structure Ib (Table III and Fig. 7) is predicted to be the most stable, and its formation can explain the observed DEA signal ($m/z = 67$ in Fig. 4) peaked at 1.0 eV. Provided that the H atom at the C(4) site is abstracted simultaneously to those at the C(3) and C(5) sites due to the same vibrational motion of the I^- anion, the $[I-3H]^-$ fragment with the linear structure Ic can be formed along with the H_2 and $H^\bullet$ neutral species with a calculated threshold as low as 0.63 eV (Table III), thus accounting for the $m/z = 66$ signals peaking at higher energies (3.8 and 5.5 eV). These two channels leading to formation of $[I-2H]^-$ and $[I-3H]^-$ were not observed in previous studies of DEA to isoxazole due to much lower sensitivity than in the present study [21].

The present B3LYP/6-31+G(d) calculations predict that migration of an H atom from N(1) to the adjacent positions C(2) and C(5) in molecular anions of imidazole and pyrazole, respectively, leads to a stabilization of 0.36 and 0.01 eV with respect to the parent anions with the structures of imidazole and pyrazole displayed in Fig. 1. This result is in line with the supposed high mobility of hydrogen atoms in II^- and III^- that should make their elimination easier, especially in the H_2 form. In contrast to I, H atom stripping in II–IV likely cannot occur in one step since an out-of-plane vibration which stimulates ring opening and simultaneously moves two hydrogen atoms closer to each other is not present. As a further comment for the imidazole and pyrazole anions, the most stable structure which can be formed by elimination of two hydrogen atoms accompanied by ring opening is malononitrile $CH_2(CN)_2$. Interestingly, another study showed a possibility of loss of 4H from imidazole as the least abundant channel out of the all dehydrogenation reactions [22]. The calculated reaction enthalpies proposed the formation of $H_2 + 2H$ and the loss of four hydrogen atoms as two channels leading to $[II-4H]^-$ and the ring opening [22].

Formation of structure IIIa (Fig. 7 and Table III) is associated with a threshold as low as 0.7 eV, thus accounting for the presence of the $[III-2H]^-$ signal. In turn, the $[M-3H]^-$ species (M = II or III) can be associated with a negatively charged dehydrogenated malononitrile radical (IIIb in Fig. 7), whose EA has been estimated to be 2.88 eV [85]. This decay can originate via elimination of H_2 from the $[III-H]^-$ species, dehydrogenated at the N site, favored by the in-plane vibration represented in Fig. 7 (eighth normal mode, B3LYP/6-31+G(d) frequency = 1033.24 cm^{-1}). This vibration moves the two H atoms closer to each other and simultaneously elongates the N–N bond stimulating ring opening. Formation of an analogous malononitrilelike structure in II is less probable, because it would require complex rearrangements, including exchanged positions of C and N atoms.

H atom stripping and ring opening in pyrrole can involve formation of a negative ion with cyanopropynelike structure (IVa) and its dehydrogenated form (IVb) that requires migration of only light H atoms, thus producing the lowest DEA thresholds (see Table III). However, formation of the $[IV-2H]^-$ fragment with a cyclic structure by H abstraction from the adjacent N(1) and C(2) atoms requires an energy (1.98 eV) only slightly higher than that required for IVa (1.84 eV). A comparison of the present DEA findings for pyrrole with earlier data is difficult since the latter either include only individual peaks (experimental curves are interrupted between the maxima) in the DEA anion yields [86] or report only the most intense signals [87]. Likely due to methylation at the N(1) site in V, the $[V-2H]^-$ anion is not observed, but $[VI-2H]^-$ decay becomes available in VI, providing evidence for involvement of the N(1) hydrogen atom in this decay. The spectrum for the $[V-2H-CH_3]^-$ negative fragment ($m/z = 65$) presents some analogy to the one for H atom stripping and represents an alternative observed way of demethylation of V by low-energy electrons.

E. Other decay channels in the DEA cross section

At high incident electron energies, the DEA spectra of all studied compounds display common signals associated with negative fragments generated by ring cleavage. For instance, the CN^- current ($m/z = 26$, see Figs. 4–6) is observed in I–IV and VI with relatively high intensity, this decay channel being likely associated with ring cleavage and atomic rearrangements in the neutral counterparts, as deduced from B3LYP/6-31+G(d) calculations. Three of the more prominent channels and the possible fragment structures produced via DEA to isoxazole were reported previously and are in a good agreement with the present study [21]. The $m/z = 39$ current in the DEA spectra of I–VI can reasonably be ascribed to formation of the $HCCN^-$ anion. The EA of the corresponding neutral diradical—"unusual" triplet cyanocarbene (or cyanomethylene) molecule—has been estimated to be 2.003 ± 0.014 eV [88]. The cyanomethyl anion (CH_2CN^-), a possible interstellar species [89], is likely responsible for the $m/z = 40$ signal in II–VI, the EA of the corresponding radical being estimated as 1.53 eV [85,90].

Formation of $C_2H_3N^-$ ($m/z = 41$), observed in I–III, can be due to elimination of small neutral closed-shell CO molecules from I^- and HCN from II^- and III^-. In II and III this signal cannot be accounted for by isotopic contributions from the more abundant $m/z = 40$ fragment. Owing to the presence of oxygen in the heterocycle, DEA to I produces a series of additional fragment species not observed in the

spectra of compounds II–VI, such as OCN^- ($m/z = 42$) and C_3N^- ($m/z = 50$). The latter fragment, observed earlier in a DEA study of cyanoacetylene [91], could in principle be formed by DEA to II–VI, but it was not observed in the present experiments. Its production by DEA to I is associated with removing of all H atoms along with the oxygen atom to form H_2 and $OH^\bullet$ or H_2O and H atom as neutral counterparts. Some small anionic species (cyanomethylene, cyanopropyne, C_3N) detected in the DEA spectra of the present compounds are related to formation of nitriles in the upper atmosphere of Titan and its satellites via the DEA mechanism [91–93].

IV. CONCLUSIONS

Formation of TNI states by low-energy electron attachment and decomposition of the parent molecular negative ions via DEA are investigated in a series of five-membered heterocyclic compounds (isoxazole, imidazole, pyrazole, pyrrole, 1-methyl-, and 2-methylimidazole) which are building blocks in many biologically relevant molecules. The experimental findings obtained using ETS and DEAS are assigned with the support of quantum-chemical calculations. Multichannel ERT calculations were carried out to reproduce experimental low-energy features observed in the DEA spectra, and ascribed to long-range electron-molecule interaction. Due to the importance of electron-driven processes for understanding the effects of high-energy radiations in living tissues, this study can have an impact in the rapidly developing field of radiotherapy. The main conclusions are as follows:

(1) The energy positions of the lowest π^* VAEs measured in II–IV are in excellent agreement with previous literature data. The lowest σ^*_{N-H} anion state is predicted to lie around 3 eV, not in disagreement with the present experimental data, although not observed in the ET spectra.

(2) Very narrow (0.1 eV) "cusps" are observed around 0.45 eV in the ET spectra of II–IV, which contain an N–H bond, but not in isoxazole where this bond is absent. These features are associated with VFRs in good agreement with the results of ERT calculations.

(3) Since the position of the lowest π_1^* shape resonance matches the position of the DEA peak generated by the dehydrogenated $[M-H]^-$ negative fragment (M = II−IV and VI) it is difficult to evaluate possible contributions from mechanisms other than vibronic σ^*/π^* mixing for the elimination of a hydrogen atom via low-energy electron attachment.

(4) DEA is found to cause abstraction of as many as two and three hydrogen atoms from the heterocyclic structure of I–IV, accompanied in some cases by ring opening and formation of H atoms and H_2 molecules as neutral counterparts. Ring opening takes place when the two heteroatoms occupy adjacent positions in the ring, thus suggesting that cleavage of the covalent bond between them favors this process.

(5) H atoms are more mobile in molecular negative ions as compared with neutral molecules, in line with DFT calculations in II and III. H atom stripping can occur in one step in I since there is a specific vibration that can stimulate elimination of three H atoms accompanied by both H_2 formation and ring opening. H atom striping in III and V can lead to production of malononitrile- and cyanopropynelike fragment species, respectively.

(6) The mechanisms of H atom stripping are complex. They include rearrangements, cleavage, and formation of several covalent bonds, and also depend on the kind and position of heteroatoms in the ring. For this reason, the process is expected to be "slow," appearing on a microsecond time scale.

ACKNOWLEDGMENTS

We acknowledge P. D. Burrow (Department of Physics and Astronomy, University of Nebraska-Lincoln) for many useful comments regarding the cusp features and for providing guidance for the ETS experiments. The work was performed under the Russian Government Task No. AAAA-A19-119022290052-9. The authors are grateful to the Russian Foundation for Basic Research (Grant No. 18-03-00179) and the Italian Ministero dell'Istruzione, dell'Università e della Ricerca for financial support. I.I.F. has been supported by the U.S. National Science Foundation through Grant No. PHY-1803744. S.P. acknowledges the US Department of Energy Office of Science, Office of Basic Energy Sciences under Award No. DE-FC02-04ER15533 (NDRL No. 5239). The experiments were conducted partly using the equipment of the Research park of St. Petersburg State University "Physical methods of surface investigation."

[1] B. Boudaïffa, P. Cloutier, D. Hunting, M. A. Huels, and L. Sanche, Resonant formation of DNA strand breaks by low-energy (3 to 20 eV) electrons, Science **287**, 1658 (2000).

[2] I. I. Fabrikant, S. Eden, N. J. Mason, and J. Fedor, Recent progress in dissociative electron attachment: From diatomics to biomolecules, Adv. At. Mol. Opt. Phys. **66**, 545 (2017).

[3] J. D. Gorfinkiel and S. Ptasinska, Electron scattering from molecules and molecular aggregates of biological relevance, J. Phys. B: At. Mol. Opt. Phys. **50**, 182001 (2017).

[4] R. L. Mundy and M. H. Heiffer, The Pharmacology of radioprotectant chemicals: General pharmacology of β-mercaptoethylamine. Radiat. Res. **13**, 381 (1960).

[5] P. Paul, M. K. Unnikrishnan, and A. N. Nagappa, Phytochemicals as radioprotective agents – A review, Ind. J. Nat. Prod. Res. **2**, 137–150 (2011).

[6] M. Z. Kamran, A. Ranjan, N. Kaur, S. Sur, and V. Tandon, Radioprotective agents: Strategies and translational advances, Med. Res. Rev. **36**, 461 (2016).

[7] S. Nambiar and J. T. Yeow, Polymer-composite materials for radiation protection, ACS Appl. Mater. Inter. **4**, 5717 (2012).

[8] L. Sanche, Interaction of low energy electrons with DNA: Applications to cancer radiation therapy, Radiat. Phys. Chem. **128**, 36 (2016).

[9] E. Surdutovich, G. Garcia, N. Mason, and A. V. Solov'yov, Nano-scale processes behind ion-beam cancer therapy, Eur. Phys. J. D **70**, 86 (2016).

[10] M. Rezaee, R. P. Hill, and D. A. Jaffray, The exploitation of low-energy electrons in cancer treatment, Radiat. Res. **188**, 123 (2017).

[11] I. Baccarelli, I. Bald, F. A. Gianturco, E. Illenberger, and J. Kopyra, Electron-induced damage of DNA and its components: Experiments and theoretical models, Phys. Rep. **508**, 1 (2011).

[12] D. K. Dalvie, A. S. Kalgutkar, S. C. Khojasteh-Bakht, R. S. Obach, and J. P. O'Donnell, Biotransformation reactions of five-membered aromatic heterocyclic rings, Chem. Res. Toxicol. **15**, 269 (2002).

[13] K. Karrouchi, S. Radi, Y. Ramli, J. Taoufik, Y. Mabkhot, and F. Al-Aizari, Synthesis and pharmacological activities of pyrazole derivatives: A review, Molecules **23**, 134 (2018).

[14] I. Vujasinović, A. Paravić-Radičević, K. Mlinarić-Majerski, K. Brajša, and B. Bertoša, Synthesis and biological validation of novel pyrazole derivatives with anticancer activity guided by 3D-QSAR analysis, Bioorgan. Med. Chem. **20**, 2101 (2012).

[15] A. A. Bekhit, A. Hymete, E. D. A. Bekhit, A. Damtew, and H. Y. Aboul-Enein, Pyrazoles as promising scaffold for the synthesis of anti-inflammatory and/or antimicrobial agent: A review, Mini Rev. Med. Chem. **10**, 1014 (2010).

[16] S. A. Pshenichnyuk, A. Modelli, and A. S. Komolov, Interconnections between dissociative electron attachment and electron-driven biological processes, Int. Rev. Phys. Chem. **37**, 125 (2018).

[17] A. Modelli, M. Guerra, D. Jones, G. Distefano, K. J. Irgolic, K. Franch, and G. Pappalardo, Electron transmission spectra of selenophene and tellurophene and Xα computations of electron affinities for chalcophenes, Chem. Phys. **88**, 455 (1984).

[18] A. Modelli and P. D. Burrow, Electron attachment to the aza-derivatives of furan, pyrrole, and thiophene, J. Phys. Chem. A **108**, 5721 (2004).

[19] L. Sanche and G. J. Schulz, Electron transmission spectroscopy: Rare gases. Phys. Rev. A **5**, 1672 (1972).

[20] K. D. Jordan and P. D. Burrow, Temporary anion states of polyatomic hydrocarbons, Chem. Rev. **87**, 557 (1987).

[21] Z. Li, I. Carmichael, and S. Ptasinska, Dissociative electron attachment induced ring opening in five-membered heterocyclic compounds, Phys. Chem. Chem. Phys. **20**, 18271 (2018).

[22] A. Ribar, K. Fink, Z. Li, S. Ptasińska, I. Carmichael, L. Feketeová, and S. Denifl, Stripping off hydrogens in imidazole triggered by the attachment of a single electron, Phys. Chem. Chem. Phys. **19**, 6406 (2017).

[23] N. L. Asfandiarov, S. A. Pshenichnyuk, V. G. Lukin, I. A. Pshenichnyuk, A. Modelli, and Š. Matejčik, Temporary anion states and dissociative electron attachment to nitrobenzene derivatives, Int. J. Mass Spectrom. **264**, 22 (2007).

[24] N. L. Asfandiarov, S. A. Pshenichnyuk, R. G. Rakhmeyev, R. F. Tuktarov, N. L. Zaitsev, A. S. Vorob'ev, J. Kočišek, J. Fedor, and A. Modelli, 4-Bromobiphenyl: Long-lived molecular anion formation and competition between electron detachment and dissociation, J. Chem. Phys. **150**, 114304 (2019).

[25] P. D. Burrow, G. A. Gallup, A. M. Scheer, S. Denifl, S. Ptasinska, T. Märk, and P. Scheier, Vibrational Feshbach resonances in uracil and thymine, J. Chem. Phys. **124**, 124310 (2006).

[26] A. Pelc, W. Sailer, P. Scheier, and T. D. Märk, Generation of (M–H)− ions by dissociative electron attachment to simple organic acids M, Vacuum **78**, 631 (2005).

[27] A. Modelli, D. Jones, and S. A. Pshenichnyuk, Electron attachment to indole and related molecules, J. Chem. Phys. **139**, 184305 (2013).

[28] G. A. Gallup and I. I. Fabrikant, Vibrational Feshbach resonances in dissociative electron attachment to uracil, Phys. Rev. A **83**, 012706 (2011).

[29] V. Vizcaino, B. Puschnigg, S. E. Huber, M. Probst, I. I. Fabrikant, G. A. Gallup, E. Illenberger, P. Scheier, and S. Denifl, Hydrogen loss in aminobutanoic acid isomers by the σ^* resonance formed in electron capture, New J. Phys. **14**, 043017 (2012).

[30] M. Smyth, J. Kohanoff, and I. I. Fabrikant, Electron-induced hydrogen loss in uracil in a water cluster environment, J. Chem. Phys. **140**, 184313 (2014).

[31] A. Modelli and S. A. Pshenichnyuk, Gas-phase dissociative electron attachment to flavonoids and possible similarities to their metabolic pathways, Phys. Chem. Chem. Phys. **15**, 1588 (2013).

[32] S. A. Pshenichnyuk, N. L. Asfandiarov, and A. V. Kukhta, Interruption of the inner rotation initiated in isolated electron-driven molecular rotors, Phys. Rev. A **86**, 052710 (2012).

[33] C. Desfrançois, H. Abdoul-Carime, and J. P. Schermann, Ground-state dipole-bound anions, Int. J. Mod. Phys. B **10**, 1339 (1996).

[34] K. D. Jordan and F. Wang, Theory of dipole-bound anions. Annu. Rev. Phys. Chem. **54**, 367 (2003).

[35] C. Desfrançois, H. Abdoul-Carime, N. Khelifa, and J. P. Schermann, From $1/r$ to $1/r^2$ Potentials: Electron Exchange between Rydberg Atoms and Polar Molecules, Phys. Rev. Lett. **73**, 2436 (1994).

[36] O. H. Crawford, Negative ions of polar molecules, Mol. Phys. **20**, 585 (1971).

[37] A. Schramm, I. I. Fabrikant, J. M. Weber, E. Leber, M. W. Ruf, and H. Hotop, Vibrational resonance and threshold effects in inelastic electron collisions with methyl iodide molecules, J. Phys. B: At. Mol. Opt. Phys. **32**, 2153 (1999).

[38] R. S. Wilde, G. A. Gallup, and I. I. Fabrikant, Comparative studies of dissociative electron attachment to methyl halides. J. Phys. B: At. Mol. Opt. Phys. **33**, 5479 (2000).

[39] J. M. Weber, I. I. Fabrikant, E. Leber, M. W. Ruf, and H. Hotop, Effects of solvation on dissociative electron attachment to methyl iodide clusters, Eur. Phys. J. D **11**, 247 (2000).

[40] G. A. Gallup and I. I. Fabrikant, Resonances and threshold effects in low-energy electron collisions with methyl halides, Phys. Rev. A **75**, 032719 (2007).

[41] A. M. Scheer, K. Aflatooni, G. A. Gallup, and P. D. Burrow, Bond Breaking and Temporary Anion States in Uracil and Halouracils: Implications for the DNA Bases, Phys. Rev. Lett. **92**, 068102 (2004).

[42] Z. Li, M. Ryszka, M. M. Dawley, I. Carmichael, K. B. Bravaya, and S. Ptasińska, Dipole-Supported Electronic Resonances Mediate Electron-Induced Amide Bond Cleavage, Phys. Rev. Lett. **122**, 073002 (2019).

[43] I. C. Walker, M. H. Palmer, M. J. Hubin-Franskin, and J. Delwiche, VUV optical-absorption and near-threshold electron energy-loss spectra of pyrazole, Chem. Phys. Lett. **367**, 517 (2003).

[44] I. C. Walker, M. H. Palmer, J. Delwiche, S. V. Hoffmann, P. L. Vieora, N. J. Mason, M. F. Guest, M.-J. Hubin-Franskin, and A. Giuliani, The electronic states of isoxazole studied by VUV absorption, electron energy-loss spectroscopies and *ab initio* multi-reference configuration interaction calculations, Chem. Phys. **297**, 289 (2004).

[45] W. R. Garrett, Low-energy electron scattering by polar molecules, Mol. Phys. **24**, 465 (1972).

[46] I. I. Fabrikant, Long-range effects in electron scattering by polar molecules, J. Phys. B: At. Mol. Opt. Phys. **49**, 222005 (2016).

[47] K. Aflatooni, G. A. Gallup, and P. D. Burrow, Temporary anion states of dichloroalkanes and selected polychloroalkanes, J. Phys. Chem. A **104**, 7359 (2000).

[48] A. Stamatovic and G. J. Schulz, Characteristics of the trochoidal electron monochromator, Rev. Sci. Instrum. **41**, 423 (1970).

[49] G. J. Schulz, Resonances in electron impact on diatomic molecules, Rev. Mod. Phys. **45**, 423 (1973).

[50] V. I. Khvostenko, *Negative Ion Mass Spectrometry in Organic Chemistry* (Nauka, Moscow, 1981) (in Russian).

[51] L. G. Christophorou, *Electron-Molecule Interactions and Their Applications* (Academic, Orlando, 1984).

[52] M. Allan, Study of triplet states and short-lived negative ions by means of electron impact spectroscopy, J. Electron. Spectrosc. Relat. Phenom. **48**, 219 (1989).

[53] E. Illenberger and J. Momigny, *Gaseous Molecular Ions. An Introduction to Elementary Processes Induced by Ionization* (Springer-Verlag, New York, 1992).

[54] S. A. Pshenichnyuk and A. Modelli, in *Mitochondrial Medicine: Volume II, Manipulating Mitochondrial Function, Methods in Molecular Biology*, edited by V. Weissig and M. Edeas (Springer Science + Business Media, New York, 2015), Vol. 1265, p. 285.

[55] M. W. Schmidt, K. K. Baldridge, J. A. Boatz, S. T. Elbert, M. S. Gordon, J. H. Jensen, S. Koseki, N. Matsunaga, K. A. Nguyen, S. J. Su, T. L. Windus, M. Dupuis, and J. A. Montgomery, J. Comput. Chem. **14**, 1347 (1993); see also http://www.msg.ameslab.gov/GAMESS/GAMESS.html.

[56] D. Chen and G. A. Gallup, The relationship of the virtual orbitals of self-consistent-field theory to temporary negative ions in electron scattering from molecules, J. Chem. Phys. **93**, 8893 (1990).

[57] S. W. Staley and J. T. Strnad, Calculation of the energies of π^* negative ion resonance states by the use of Koopmans' theorem, J. Phys. Chem. **98**, 116 (1994).

[58] A. Modelli, Electron attachment and intramolecular electron transfer in unsaturated chloroderivatives, Phys. Chem. Chem. Phys. **5**, 2923 (2003).

[59] A. M. Scheer and P. D. Burrow, π^* Orbital system of alternating phenyl and ethynyl groups: Measurements and calculations, J. Phys. Chem. B **110**, 17751 (2006).

[60] M. J. Frisch, G. W. Trucks, H. B. Schlegel, G. E. Scuseria, M. A. Robb, J. R. Cheeseman, G. Scalmani, V. Barone, B. Mennucci, and G. A. Petersson *et al.*, *Gaussian 09, Revision A.02* (Gaussian, Inc., Wallingford CT, 2009).

[61] I. I. Fabrikant, H. Hotop, and M. Allan, Elastic scattering, vibrational excitation, and attachment in low-energy electron-SF_6 scattering: Experiment and effective range theory, Phys. Rev. A **71**, 022712 (2005).

[62] J. P. Gauyacq and A. Herzenberg, The attachment of very slow electrons to polyatomic molecules, J. Phys. B: At. Mol. Phys. **17**, 1155 (1984).

[63] M. Allan, M. Lacko, P. Papp, Š. Matejčík, M. Zlatar, I. I. Fabrikant, J. Kočišek, and J. Fedor, Dissociative electron attachment and electronic excitation in $Fe(CO)_5$, Phys. Chem. Chem. Phys. **20**, 11692 (2018).

[64] L. D. Landau and E. M. Lifshitz, *Quantum Mechanics (Nonrelativistic Theory)* (Butterworth-Heinemann, Oxford, 1981).

[65] W. Domcke, Theory of resonance and threshold effects in electron-molecule collisions: The projection-operator approach, Phys. Rep. **208**, 97 (1991).

[66] H. Hotop, M. W. Ruf, M. Allan, and I. I. Fabrikant, Resonance and threshold phenomena in low-energy electron collisions with molecules and clusters, Adv. At. Mol. Opt. Phys. **49**, 85 (2003).

[67] D. Christen, J. H. Griffiths, and J. Sheridan, The microwave spectrum of imidazole; complete structure and the electron distribution from nuclear quadrupole coupling tensors and dipole moment orientation, Z. Naturforsch. A **36**, 1378 (1981).

[68] W. H. Kirchhoff, The microwave spectrum and dipole moment of pyrazole, J. Am. Chem. Soc. **89**, 1312 (1967).

[69] U. Nygaard, J. T. Nielsen, J. Kirchheiner, G. Maltesen, J. Rastrup-Andersen, and G. O. Sørensen, Microwave spectra of isotopic pyrroles. Molecular structure, dipole moment, and 14N quadrupole coupling constants of pyrrole, J. Mol. Struct. **3**, 491 (1969).

[70] K. E. Calder, R. L. Calvert, P. B. Lukins, and G. L. D. Ritchie, Magnetic anisotropies and relative aromaticities of pyrrole, pyrazole, imidazole and their N-methyl derivatives, Aust. J. Chem. **34**, 1835 (1981).

[71] C. Perchard, A. M. Bellocq, and A. Novak, Spectres de vibration de l'imidazole, de l'imidazole (D) – 1, de l'imidazole (D3)-2,4,5 et de l'imidazole (D4) – Partie II. —Région entre 1700 et 30 cm^{-1}, J. Chim. Phys. **62**, 1344 (1965).

[72] M. Majoube, Vibrational spectra of pyrazole and deuterium-substituted analogues, J. Raman Spectrosc. **20**, 49 (1989).

[73] T. D. Klots, R. D. Chirico, and W. V. Steele, Complete vapor phase assignment for the fundamental vibrations of furan, pyrrole and thiophene, Spectrochim. Acta A: Mol. Spectrosc. **50**, 765 (1994).

[74] L. M. Culberson, C. C. Blackstone, R. Wysocki, and A. Sanov, Selective deprotonation of oxazole and photoelectron imaging of the oxazolide anion, Phys. Chem. Chem. Phys. **16**, 527 (2014).

[75] T. Skalický, C. Chollet, N. Pasquier, and M. Allan, Properties of the π^* and $\sigma*$ states of the chlorobenzene anion determined by electron impact spectroscopy, Phys. Chem. Chem. Phys. **4**, 3583 (2002).

[76] K. Aflatooni, A. M. Scheer, and P. D. Burrow, Total dissociative electron attachment cross sections for molecular constituents of DNA, J. Chem. Phys. **125**, 054301 (2006).

[77] G. A. Gallup, P. D. Burrow, and I. I. Fabrikant, Electron-induced bond breaking at low energies in HCOOH and glycine: The role of very short-lived $\sigma*$ anion states, Phys. Rev. A **79**, 042701 (2009).

[78] Y. V. Vasil'ev, B. J. Figard, D. F. Barofsky, and M. L. Deinzer, Resonant electron capture by some amino acids esters, Int. J. Mass Spectrom. **268**, 106 (2007).

[79] J. Kocisek, P. Papp, P. Mach, Y. V. Vasil'ev, M. L. Deinzer, and S. Matejčík, Resonance electron capture by serine, J. Phys. Chem. A **114**, 1677 (2009).

[80] S. A. Pshenichnyuk and A. S. Komolov, Dissociative electron attachment to resveratrol as a likely pathway for generation of the H_2 antioxidant species inside mitochondria, J. Phys. Chem. Lett. **6**, 1104 (2015).

[81] S. A. Pshenichnyuk, Y. N. Elkin, N. I. Kulesh, E. F. Lazneva, and A. S. Komolov, Low-energy electron interaction with retusin extracted from Maackia amurensis: Towards a molecular mechanism of the biological activity of flavonoids, Phys. Chem. Chem. Phys. **17**, 16805 (2015).

[82] Y. V. Vasil'ev, B. J. Figard, V. G. Voinov, D. F. Barofsky, and M. L. Deinzer, Resonant electron capture by some amino acids and their methyl esters, J. Am. Chem. Soc. **128**, 5506 (2006).

[83] S. Denifl, H. D. Flosadóttir, A. Edtbauer, O. Ingólfsson, T. D. Märk, and P. Scheier, A detailed study on the decomposition pathways of the amino acid valine upon dissociative electron attachment, Eur. Phys. J. D **60**, 37 (2010).

[84] V. Vizcaino, P. Bartl, D. Gschliesser, S. E. Huber, M. Probst, T. D. Märk, P. Scheier, and S. Denifl, Dissociative electron attachment to β-alanine, Chem. Phys. Chem. **12**, 1272 (2011).

[85] D. J. Goebbert, L. Velarde, D. Khuseynov, and A. Sanov, C−H bond dissociation energy of malononitrile, J. Phys. Chem. Lett. **1**, 792 (2010).

[86] M. V. Muftakhov, N. L. Asfandiarov, and V. I. Khvostenko, Resonant dissociative attachment of electrons to molecules of five-membered heterocyclic compounds and lactams, J. Electron. Spectrosc. Relat. Phenom. **69**, 165 (1994).

[87] T. Skalický and M. Allan, The assignment of dissociative electron attachment bands in compounds containing hydroxyl and amino groups, J. Phys. B: At. Mol. Opt. Phys. **37**, 4849 (2004).

[88] M. R. Nimlos, G. Davico, C. M. Geise, P. G. Wenthold, W. C. Lineberger, S. J. Blanksby, C. M. Hadad, G. A. Petersson, and G. B. Ellison, Photoelectron spectroscopy of $HCCN^-$ and $HCNC^-$ reveals the quasilinear triplet carbenes, HCCN and HCNC, J. Chem. Phys. **117**, 4323 (2002).

[89] R. C. Fortenberry, T. D. Crawford, and T. J. Lee, The possible interstellar anion CH_2CN^-: Spectroscopic constants, vibrational frequencies, and other considerations, Astrophys. J. **762**, 121 (2012).

[90] S. Moran, H. B. Ellis Jr, D. J. De Frees, A. D. McLean, and G. B. Ellison, Carbanion spectroscopy: Cyanomethide anion (CH_2CN^-), J. Am. Chem. Soc. **109**, 5996 (1987).

[91] T. D. Gilmore and T. A. Field, Absolute cross sections for dissociative electron attachment to HCCCN, J. Phys. B: At. Mol. Opt. Phys. **48**, 035201 (2015).

[92] N. Balucani, M. Alagia, L. Cartechini, P. Casavecchia, G. G. Volpi, K. Sato, T. Takayanagi, and Y. Kurosaki, Cyanomethylene formation from the reaction of excited nitrogen atoms with acetylene: A crossed beam and *ab initio* study, J. Am. Chem. Soc. **122**, 4443 (2000).

[93] F. Cerceau, F. Raulin, R. Courtin, and D. Gautier, Infrared spectra of gaseous mononitriles: Application to the atmosphere of Titan, Icarus **62**, 207 (1985).